2.5 kV Vertical Ga₂O₃ Schottky Rectifier with Graded Junction Termination Extension

Boyan Wang, Student Member, IEEE, Ming Xiao, Joseph Spencer, Yuan Qin, Kohei Sasaki, Marko J. Tadjer, Senior Member, IEEE, and Yuhao Zhang, Senior Member, IEEE

Abstract—This work demonstrates vertical Ga2O3 Schottky barrier diodes (SBDs) with a novel junction termination extension (JTE) comprising multiple layers of sputtered p-type nickel oxide (NiO). The NiO layers have the varied lengths to enable a graded decrease in effective charge density away from the main junction. The fabrication of this JTE obviates the etch or implantation and shows good throughput. The fabricated Ga2O3 SBDs exhibit a forward voltage below 1.9 V at the current density of 100 A/cm², a differential specific on-resistance of 5.9 m Ω ·cm², and a breakdown voltage over 2.5 kV. The Baliga's figure of merit (FOM) exceeds 1 GW/cm² and is among the highest in multi-kilovolt Ga2O3 SBDs. Besides, the capacitance of the JTE region is extracted, allowing for evaluation of the capacitance, charge, and switching FOM of 1.7 kV-class Ga2O3 SBDs with varied current ratings. The results show good promise of Ga2O3 SBDs for kilovolt power electronics. 1

Index Terms— power electronics, ultra-wide bandgap, gallium oxide, junction termination extension, nickel oxide, breakdown voltage, on-resistance, capacitance

I. INTRODUCTION

allium oxide (Ga_2O_3) has emerged as a promising material for future power devices, due to its ultra-wide bandgap, high critical electric field (E_C), controllable doping, and large-diameter wafer availability [1]. In various Ga_2O_3 devices, vertical Ga_2O_3 Schottky barrier diodes (SBDs) are advancing fast towards applications. Recent reports include an specific onresistance ($R_{ON,SP}$) versus breakdown voltage (BV) trade-off superior to SiC [2], as well as excellent thermal resistance and surge current capability in the packaged SBDs [3]–[5].

Edge termination is a key challenge for making high-voltage Ga_2O_3 SBDs. Junction termination extension (JTE) is dominant in industrial Si, SiC and GaN devices [6], [7], and it relies on p-n junctions formed by diffusion or implantation. As effective p-type doping is lacking in Ga_2O_3 [8], prior edge terminations for Ga_2O_3 SBDs employ trench, field plate, high-k dielectrics, and deep acceptors [2], [9]–[14]. Their processing usually requires deep etch or high temperature annealing, which could compromise the process yield, particularly for high-voltage devices. To date, only a few vertical Ga_2O_3 SBDs with BV > 2 kV have been reported [2], [10], [15].

Meanwhile, p-type nickel oxide (bandgap $3.4\sim4$ eV [8]) is recently applied to form p-n junction diodes in Ga_2O_3 . Since the first report [16], NiO/ Ga_2O_3 p-n diodes have achieved multi-kilovolt BV and low differential $R_{ON,SP}$ [17]–[22]. Whereas,

¹Manuscript received XXXX; revised XXXX. This work was supported by the National Science Foundation under Grants ECCS-2100504 and ECCS-2202620 and in part by the Center for Power Electronics Systems High Density Integration Industry Consortium. (B. Wang and M. Xiao contributed equally to this work.) (Corresponding Authors: Yuhao Zhang, Ming Xiao).

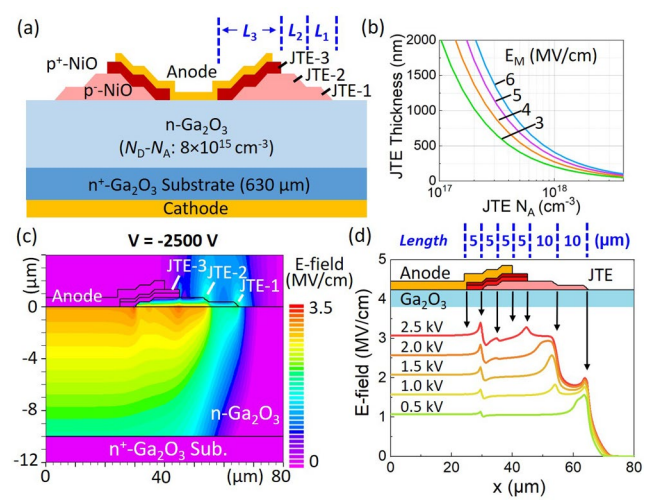


Fig. 1. (a) Schematic of the Ga_2O_3 SBD with NiO JTE. (b) Upper limits of JTE thickness versus N_A as a function of E_M . (c) Simulated E-field contour at 2500 V. (d) E-field profile in Ga_2O_3 at voltages from 0.5 to 2.5 kV.

they suffer from a high forward voltage ($V_F \sim 3$ V), leading to high conduction loss. Ga₂O₃ SBDs that combine a low V_F and the NiO/Ga₂O₃ blocking junction are thus desirable.

Single-zone, highly-doped NiO JTEs were recently applied to Ga₂O₃ SBDs [23], [24]. However, the effectiveness of single-zone JTEs is very sensitive to the JTE dose. SiC and Si research reveals that this sensitivity can be overcome by multizone JTE [25], bevel JTE [26], and graded doped JTE [6]. The key common feature of these JTEs is a gradual decrease in the effective JTE charge away from the main junction.

This work develops a novel multilayer NiO JTE with graded charge density. This JTE enables BV > 3 kV in the p-n junction. High work function (WF) metal is used in Ga₂O₃ SBDs to suppress the leakage current and exploit this JTE, enabling a BV over 2.5 kV. The capacitance and charge are also evaluated, which have been rarely reported in prior Ga₂O₃ diodes.

II. JTE DESIGN

Fig. 1(a) shows the schematic of our JTE comprising p⁻-NiO and p⁺-NiO layers. The p⁻-NiO layers (i.e., JTE-1 and -2) fulfill the main JTE functionality by achieving a full depletion close to the surface at the desired BV. The upper limit of the JTE sheet dose can be determined from the max junction field in Ga₂O₃ ($E_{\rm M}$) at BV, i.e., $qN_A^-t_A^- \leq E_M\varepsilon_N$ [6], where ε_N is the Ga₂O₃ permittivity; N_A^- and t_A^- are acceptor concentration and total

- B. Wang, M. Xiao, J. Spencer, Y. Qin, and Y. Zhang are with the Center of Power Electronics Systems, Virginia Polytechnic Institute and State University, Blacksburg, VA 24060 USA (e-mail: mxiao@vt.edu, yhzhang@vt.edu).
- J. Spencer and M. Tadjer are with the Naval Research Laboratory, Washington, DC 20375 USA.
 - K. Sasaki is with Novel Crystal Technology, Inc., Sayama 350-1328, Japan.

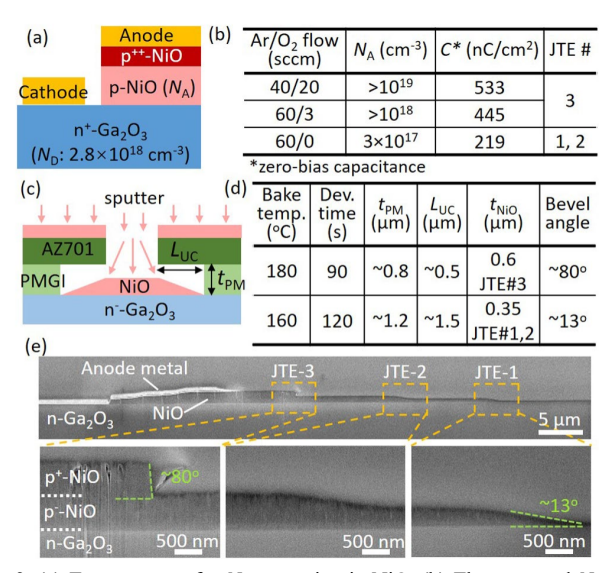


Fig. 2. (a) Test structure for N_A extraction in NiO. (b) The extracted N_A for NiO sputtered in three conditions. (c) Illustration of the NiO bevel angle formation. (d) Critical PMGI process parameters and the produced NiO bevel angle. (e) Cross-sectional SEM images of the entire JTE and each JTE.

thickness of p⁻-NiO layers, respectively. The calculated N_A^- and t_A^- upper limits as a function of E_M (from 3 to 6 MV/cm) is shown in Fig. 1(b). Note that the high N_A in many prior NiO JTEs is expected to induce a NiO partial depletion and electric field (E-field) crowding at the outmost edge.

The p⁺-NiO layers are designed to a) avoid the NiO punchthrough, b) shield the Schottky metal from high E-field, c) serve as a non-depleted JTE (i.e., JTE-3), which can reduce the Efield at the top surface of p⁻-NiO JTEs, and d) facilitate the charge extraction and supply for p⁻-NiO during switching.

The total length of each NiO layer is designed to decrease from bottom to the top. This enables a graded decrease in charge density to minimize the depletion curvature in Ga_2O_3 . From the BV standpoint, the total length of JTE-3 (L_3) and its sub-section lengths are less critical, as the depletion in JTE-3 is little and the potential drop in Ga_2O_3 below JTE-3 is relatively small. By contrast, the incremental length of the JTE-2 (L_2) and JTE-1 (L_1) [see Fig. 1(a)] are critical for spreading the E-field both at the NiO top surface and in the Ga_2O_3 below NiO.

Fig. 1(c)-(d) show the simulated E-field contour in the NiO JTE fabricated in this work. The p⁻-NiO JTE-1 and JTE-2 are depleted at 0.5 and 1 kV successively and effectively spread the E-field at higher voltages. The p⁺-NiO JTE-3 confines the high E-field within itself from reaching the Schottky metal. As voltage increases, the peak E-field location migrates from the JTE's outer edge towards its inner edge.

III. DEVICE FABRICATION

The wafer consists of a 10 μ m n-Ga₂O₃ drift layer on 630 μ m 2-inch n⁺-Ga₂O₃ substrate. C-V measurement reveal a net donor concentration (N_D - N_A) of 8×10¹⁵ cm⁻³ in n-Ga₂O₃. The device fabrication starts from the backside Ohmic contact (Ti/Au).

Two p⁻-NiO layers are then sputtered by the RF magnetron sputtering at room temperature using the NiO target (RF power 100 W). The NiO conductivity is known to positively correlate to the oxygen partial pressure in sputtering [27]. Hence, we use the pure Ar atmosphere (60 sccm) for p⁻-NiO sputtering. The

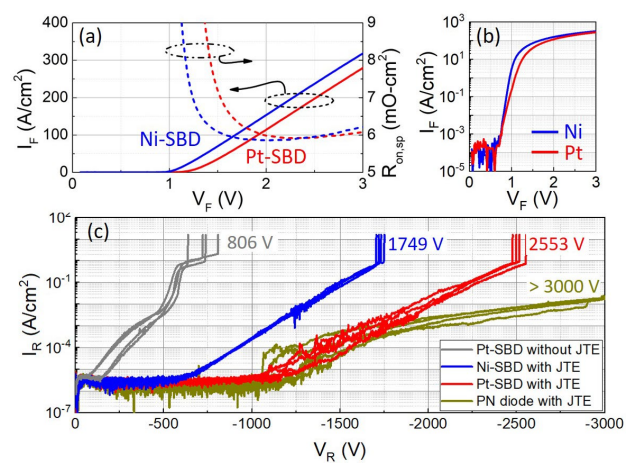


Fig. 3. Forward I-V characteristics in (a) linear and (b) semi-log scale. (c) Reverse I-V characteristics of non-JTE SBDs, Pt-SBDs, Ni-SBDs, and PNDs. Four devices at different sample locations are shown for each device type.

thickness of each p⁻-NiO layer is 350 nm. The p⁺-NiO layers are sputtered in one lift-off step consisting of 350 nm NiO in Ar/O₂ of 60/3 sccm and 250 nm NiO in Ar/O₂ of 40/20 sccm. The gradual $N_{\rm A}$ increase in p⁺-NiO minimizes the E-field crowding. After the post-sputter annealing at 275 °C in N₂, two types of Schottky metal stacks, the Pt/Au and Ni/Au, are deposited, followed by a final annealing at 225 °C in N₂.

To probe the N_A , NiO is also sputtered on n⁺-Ga₂O₃ substrate in the above three atmospheres, followed by the fabrication of the C-V test structures (Fig. 2(a)). This n⁺-p⁻ junction favors the extraction of N_A . From the capacitance, the N_A is extracted as 3×10^{17} cm⁻³, $> 10^{18}$ cm⁻³, and $> 10^{19}$ cm⁻³ for Ar/O₂ = 60/0, 60/3, and 40/20 sccm, respectively, as detailed in Fig. 2(b).

A bi-layer resist (AZ701/PMGI) is used for NiO lift-offs similar to [28]. The NiO bevel angle depends on the PMGI's undercut length ($L_{\rm UC}$) and the sputtered NiO thickness ($t_{\rm NiO}$) (Fig. 2(c)). A larger $L_{\rm UC}$ can be tuned by reducing the PMGI's bake temperature and increasing the develop time. On the other hand, a larger PMGI thickness ($t_{\rm PM}$) can facilitate the NiO sputtering into the undercut. By using the parameters listed in Fig. 2(d), the angles of p⁺-NiO layer (JTE-3) and p⁻-NiO layers (JTE-1 and -2) are engineered to be ~80° and ~13°, respectively, as shown in the scanning electron microscopy (SEM) image (Fig. 2(e)). The small angle in p⁻-NiO can reduce the surface Efield. For JTE-3, as no high E-field is present at the edge of the barely depleted p⁺-NiO, a small angle is not needed.

The total JTE length ($L_{\rm JTE}$) is 40 µm, with L_1 , L_2 and L_3 being 10 µm, 10 µm and 20 µm, respectively (Fig. 1(d)). Simulation reveals that, as L_2 increases, the peak E-field in Ga₂O₃ below the outer edge of JTE-3 first reduces and then saturates. It drops below the E-field near the JTE inner edge for $L_2 \ge 10$ µm.

In addition to SBDs, NiO/Ga₂O₃ p-n diodes (PNDs) with the same JTE and p-NiO region (600 nm p⁺-NiO and 700 nm p⁻-NiO) are fabricated to evaluate the JTE's true *BV*.

IV. DEVICE CHARACTERISTICS

Fig. 3(a) and (b) show forward I-V characteristics of the fabricated Pt-SBDs and Ni-SBDs with JTEs. Current density is normalized to the anode Schottky area. The turn-on voltages of Pt-SBDs and Ni-SBDs are 1.25 V and 1 V, respectively, leading to a $V_{\rm F}$ of 1.9 V and 1.7 V extracted at a forward current density ($J_{\rm F}$) of 100 A/cm². The differential $R_{\rm ON,SP}$ of two SBDs are both

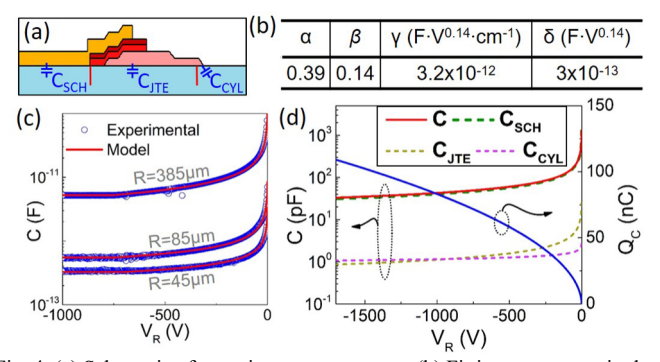


Fig. 4. (a) Schematic of capacitance components. (b) Fitting parameters in the capacitance model. (c) The experimental and modeled C-V characteristics for SBDs with various radii. (d) The projected C-V and Q-V characteristics for 1.7kV/5A SBDs. The three capacitance components are also shown.

5.9 m Ω ·cm², which is dominated by the drift region (5.2 m Ω ·cm² estimated based on a mobility of 150 cm²/Vs). The Schottky barrier height (ϕ_{SSh}) of Pt-SBDs and Ni-SBDs is estimated to be 1.35 and 1.1 eV, respectively.

Fig. 3(c) shows the reverse I-V characteristics of the Pt-SBDs, Ni-SBDs, PNDs, and SBDs without JTE. Four devices at different locations of the sample are shown for each type. Nearly all fabricated devices show good blocking capabilities, suggesting good throughput of the etch-free JTE process. The PNDs show a BV over 3 kV. The Pt-SBDs and Ni-SBDs show a BV of 2.5 kV and 1.75 kV, respectively, both being higher than the BV of SBDs without JTE (0.8 kV).

The breakdown spot in SBDs is observed at the inner JTE edge instead of the outer edge. These results validate the JTE's effectiveness and the full depletion of JTE-1 and JTE-2. The *BV* are all destructive occurring at a similar leakage current level, indicating an electrothermal failure at the Schottky edge.

The higher BV of Pt-SBDs than Ni-SBDs supports the theory in [29]: with effective edge termination, the leakage current is controlled by ϕ_{SSh} , leading to a BV (defined at a leakage current density) tradeoff with ϕ_{SSh} . Hence, in SBDs, high WF metal is desirable to exploit the high JTE BV. The average junction Efield reaches 3.08 MV/cm in Pt-SBDs at BV.

Capacitance is key for the switching performance of power devices. Experimental C-V data of SBDs with various radii (R) are fitted by the model below for capacitances of the Schottky junction (C_{Sch}), JTE (C_{JTE}), and cylindrical spreading region (C_{CYL}) (Fig. 4(a)-(c)). The C_{CYL} is proportional to perimeter and can be fitted by the power law of the reverse bias (V_{R}) [30]

$$C = C_{SSh} + C_{JJJ} + C_{CCC} = \pi R^2 \mathbb{E}_{2(\phi \stackrel{PR}{bb} + V_R)} + \pi (2\alpha R L_{JJJ} + \alpha^2 L_{JJJ}^2) \mathbb{E}_{2(\phi \stackrel{ND}{bb} + V_R)(\varepsilon_P N_A^{-1} + \varepsilon_N N_D)} + \frac{\gamma^2 \pi \mathbb{E}_R + C_{JJJ} \mathbb{E} + \delta}{(\phi_{bb}^{NbN} + V_R)(\varepsilon_P N_A^{-1} + \varepsilon_N N_D)} + \frac{\gamma^2 \pi \mathbb{E}_R + C_{JJJ} \mathbb{E} + \delta}{(\phi_{bb}^{NbN} + V_R)^\beta}$$
 (1) where ϕ_{bb}^{PP} (1.2 V) and ϕ_{bb}^{NbN} (1.7 V) is the built-in potential of the Schottly and PN imposion, representively ε_R is the NiO.

where ϕ_{bb}^{PP} (1.2 V) and ϕ_{bb}^{NBN} (1.7 V) is the built-in potential of the Schottky and PN junction, respectively. ε_P is the NiO permittivity. α accounts for the effective L_{JTE} for C_{JJJ} . β , γ , and δ are three additional fitting parameters. Their fitted values are listed in Fig. 4(b). This equation depicts the C-V characteristics before the full depletion of the drift region (at $V_R \sim 750$ V); after that, C is nearly unchanged.

The model allows one to project the capacitance and charge $(Q_{\rm C})$ of SBDs with various current ratings. Assuming the 100

TABLE I. Structural and metrics comparison of >2 kV Ga₂O₃ power diodes.

Device	Ref	Termination	V _F ^(a) (V)	$R_{ m ON,SP} \over ({ m m}\Omega{ m cm}^2)$	$I_{\rm R}^{\rm (b)}$ (A/cm ²)	BV (kV)	$C, Q_C^{(c)}$
PND	[21]	N/A N/A	2.7	2.5 11.3	6×10 ⁻² 2×10 ⁻²	2.6 4.7	
SBD	[20] [15]	field plate (FP)	3.6 N/A	250	10-2	2.3	N/A
	[10]	FP + trench	2.4	8.8	5×10^{-5}	2.89	
	[2]	FP + trench	2	3.4	10^{-6}	6	
	[31]	lateral device	$>3^{(d)}$	24.3	3×10^{-4}	3	
This work (SBD)		JTE	1.9	5.9	10-3	2.5	1.22 nF/cm ²
		Prj. 1.7kV/5A ^(e)	1.9	5.9	50 μΑ	2.5	49 pF, 120 nC

^(a) at 100 A/cm^2 forward current. ^(b) reverse current (density) at 1700 V. ^(c) C at 1700 V, Q_C integrated up to 1700 V. ^(d) 50 A/cm^2 forward current at 3 V. ^(e) projected performance of a 1.7kV/5A rated device.

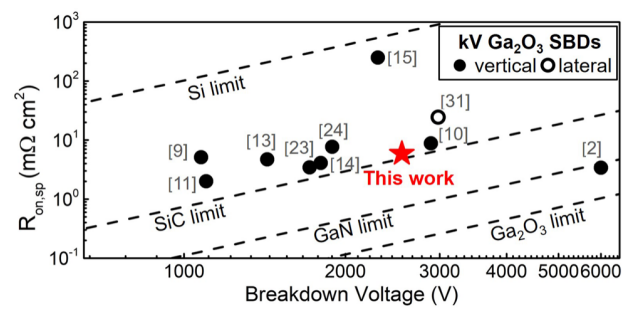


Fig. 5. Differential $R_{ON,SP}$ vs. BV trade-off of Ga_2O_3 SBDs with BV > 1 kV.

A/cm² $J_{\rm F}$ at the rated current (enabled by good packaging [4]), the C and $Q_{\rm C}$ of 1.7 kV, 5 A rated Pt-SBDs are derived (Fig. 4(d)). The $C_{\rm JTE}$ is below 5% of the total C, suggesting the advantage of the JTE as compared to other terminations (e.g., high-k field plate). The projected switching FOM ($V_{\rm F}$ · $Q_{\rm C}$) is 228 nC·V. To our best knowledge, such information is first reported for Ga₂O₃ diodes, allowing for the comparison with other diode technologies and guiding the future device applications.

Table I benchmarks the key metrics of Ga_2O_3 diodes with BV over 2 kV [2], [10], [15], [20], [21], [31]. As many diodes show a good promise for the 1.7 kV rating, the leakage current, junction capacitance and charges are extracted at the 1.7 kV or integrated up to 1.7 kV. With an implant- and etch-free process, our Pt-SBDs show the lowest V_F and a lower leakage current than PNDs. The Baliga's FOM is >1 GW/cm² and among the highest in kilovolt Ga_2O_3 SBDs (Fig. 5).

V. SUMMARY

This work demonstrates a multi-layer NiO JTE that allows for a graded decrease in charge density away from the junction. The fabrication of this NiO JTE does not require deep etch and implantation in Ga_2O_3 . Vertical Ga_2O_3 SBDs with such JTE demonstrate a BV over 2.5 kV, a low V_F and $R_{\rm ON,SP}$, and excellent static and switching FOMs. These results show the good promise of the NiO/ Ga_2O_3 p-n junction for boosting the performance of Ga_2O_3 SBDs for kilovolt power electronics.

REFERENCES

- [1] S. J. Pearton, J. Yang, P. H. Cary, F. Ren, J. Kim, M. J. Tadjer, and M. A. Mastro, "A review of Ga2O3 materials, processing, and devices," Appl. Phys. Rev., vol. 5, no. 1, p. 011301, Jan. 2018, doi: 10.1063/1.5006941.
- [2] P. Dong, J. Zhang, Q. Yan, Z. Liu, P. Ma, H. Zhou, and Y. Hao, "6 kV/3.4 mΩ·cm2 Vertical β-Ga2O3 Schottky Barrier Diode With BV2/Ron,sp Performance Exceeding 1-D Unipolar Limit of GaN and SiC," *IEEE Electron Device Lett.*, vol. 43, no. 5, pp. 765–768, May 2022, doi: 10.1109/LED.2022.3160366.
- [3] M. Xiao, B. Wang, J. Liu, R. Zhang, Z. Zhang, C. Ding, S. Lu, K. Sasaki, G.-Q. Lu, C. Buttay, and Y. Zhang, "Packaged Ga2O3 Schottky Rectifiers With Over 60-A Surge Current Capability," *IEEE Trans. Power Electron.*, vol. 36, no. 8, pp. 8565–8569, Aug. 2021, doi: 10.1109/TPEL.2021.3049966.
- [4] B. Wang, M. Xiao, J. Knoll, C. Buttay, K. Sasaki, G.-Q. Lu, C. Dimarino, and Y. Zhang, "Low Thermal Resistance (0.5 K/W) Ga₂O₃ Schottky Rectifiers With Double-Side Packaging," *IEEE Electron Device Lett.*, vol. 42, no. 8, pp. 1132–1135, Aug. 2021, doi: 10.1109/LED.2021.3089035.
- [5] H. Gong, F. Zhou, X. Yu, W. Xu, F.-F. Ren, S. Gu, H. Lu, J. Ye, and R. Zhang, "70-µm-Body Ga2O3 Schottky Barrier Diode With 1.48 K/W Thermal Resistance, 59 A Surge Current and 98.9% Conversion Efficiency," *IEEE Electron Device Lett.*, vol. 43, no. 5, pp. 773–776, May 2022, doi: 10.1109/LED.2022.3162393.
- [6] A. V. Bolotnikov, P. G. Muzykov, Q. Zhang, A. K. Agarwal, and T. S. Sudarshan, "Junction Termination Extension Implementing Drive-in Diffusion of Boron for High-Voltage SiC Devices," *IEEE Trans. Electron Devices*, vol. 57, no. 8, pp. 1930–1935, 2010, doi: 10.1109/TED.2010.2051246.
- [7] J. Liu, M. Xiao, R. Zhang, S. Pidaparthi, C. Drowley, L. Baubutr, A. Edwards, H. Cui, C. Coles, and Y. Zhang, "Trap-Mediated Avalanche in Large-Area 1.2 kV Vertical GaN p-n Diodes," *IEEE Electron Device Lett.*, vol. 41, no. 9, pp. 1328–1331, Sep. 2020, doi: 10.1109/LED.2020.3010784.
- [8] J. A. Spencer, A. L. Mock, A. G. Jacobs, M. Schubert, Y. Zhang, and M. J. Tadjer, "A review of band structure and material properties of transparent conducting and semiconducting oxides: Ga2O3, Al2O3, In2O3, ZnO, SnO2, CdO, NiO, CuO, and Sc2O3," Appl. Phys. Rev., vol. 9, no. 1, p. 011315, Mar. 2022, doi: 10.1063/5.0078037.
- [9] K. Konishi, K. Goto, H. Murakami, Y. Kumagai, A. Kuramata, S. Yamakoshi, and M. Higashiwaki, "1-kV vertical Ga2O3 field-plated Schottky barrier diodes," *Appl. Phys. Lett.*, vol. 110, no. 10, p. 103506, Mar. 2017, doi: 10.1063/1.4977857.
- [10] W. Li, K. Nomoto, Z. Hu, D. Jena, and H. G. Xing, "Field-Plated Ga2O3 Trench Schottky Barrier Diodes With a BV²/Ron,sp of up to 0.95 GW/cm2," *IEEE Electron Device Lett.*, vol. 41, no. 1, pp. 107– 110, Jan. 2020, doi: 10.1109/LED.2019.2953559.
- [11] N. Allen, M. Xiao, X. Yan, K. Sasaki, M. J. Tadjer, J. Ma, R. Zhang, H. Wang, and Y. Zhang, "Vertical Ga₂O₃ Schottky Barrier Diodes With Small-Angle Beveled Field Plates: A Baliga's Figure-of-Merit of 0.6 GW/cm²," *IEEE Electron Device Lett.*, vol. 40, no. 9, pp. 1399–1402, Sep. 2019, doi: 10.1109/LED.2019.2931697.
- [12] S. Roy, A. Bhattacharyya, P. Ranga, H. Splawn, J. Leach, and S. Krishnamoorthy, "High-k Oxide Field-Plated Vertical (001) β-Ga2O3 Schottky Barrier Diode With Baliga's Figure of Merit Over 1 GW/cm2," *IEEE Electron Device Lett.*, vol. 42, no. 8, pp. 1140–1143, Aug. 2021, doi: 10.1109/LED.2021.3089945.
- [13] C.-H. Lin, Y. Yuda, M. H. Wong, M. Sato, N. Takekawa, K. Konishi, T. Watahiki, M. Yamamuka, H. Murakami, Y. Kumagai, and M. Higashiwaki, "Vertical Ga2O3 Schottky Barrier Diodes With Guard Ring Formed by Nitrogen-Ion Implantation," *IEEE Electron Device Lett.*, vol. 40, no. 9, pp. 1487–1490, Sep. 2019, doi: 10.1109/LED.2019.2927790.
- [14] Q. He, X. Zhou, Q. Li, W. Hao, Q. Liu, Z. Han, K. Zhou, C. Chen, J. Peng, G. Xu, X. Zhao, X. Wu, and S. Long, "Selective High-Resistance Zones Formed by Oxygen Annealing for β-GaO Schottky Diode Applications," *IEEE Electron Device Lett.*, vol. 43, no. 11, pp. 1933–1936, Nov. 2022, doi: 10.1109/LED.2022.3205326.
- [15] J. Yang, F. Ren, M. Tadjer, S. J. Pearton, and A. Kuramata, "2300V Reverse Breakdown Voltage Ga2O3 Schottky Rectifiers," ECS J. Solid State Sci. Technol., vol. 7, no. 5, pp. Q92–Q96, Jan. 2018, doi: 10.1149/2.0241805jss.

- [16] Y. Kokubun, S. Kubo, and S. Nakagomi, "All-oxide p—n heterojunction diodes comprising p-type NiO and n-type β-Ga2O3," Appl. Phys. Express, vol. 9, no. 9, p. 091101, Aug. 2016, doi: 10.7567/APEX.9.091101.
- [17] H. H. Gong, X. H. Chen, Y. Xu, F.-F. Ren, S. L. Gu, and J. D. Ye, "A 1.86-kV double-layered NiO/β-Ga2O3 vertical p-n heterojunction diode," *Appl. Phys. Lett.*, vol. 117, no. 2, p. 022104, Jul. 2020, doi: 10.1063/5.0010052.
- [18] X. Lu, X. Zhou, H. Jiang, K. W. Ng, Z. Chen, Y. Pei, K. M. Lau, and G. Wang, "1-kV Sputtered p-NiO/n-Ga2O3 Heterojunction Diodes With an Ultra-Low Leakage Current Below 1 μA/cm2," *IEEE Electron Device Lett.*, vol. 41, no. 3, pp. 449–452, Mar. 2020, doi: 10.1109/LED.2020.2967418.
- [19] Y. Wang, H. Gong, Y. Lv, X. Fu, S. Dun, T. Han, H. Liu, X. Zhou, S. Liang, J. Ye, R. Zhang, A. Bu, S. Cai, and Z. Feng, "2.41 kV Vertical P-Nio/n-Ga2O3 Heterojunction Diodes With a Record Baliga's Figure-of-Merit of 5.18 GW/cm2," *IEEE Trans. Power Electron.*, vol. 37, no. 4, pp. 3743–3746, Apr. 2022, doi: 10.1109/TPEL.2021.3123940.
- [20] J.-S. Li, C.-C. Chiang, X. Xia, T. J. Yoo, F. Ren, H. Kim, and S. J. Pearton, "Demonstration of 4.7 kV breakdown voltage in NiO/β-Ga2O3 vertical rectifiers," *Appl. Phys. Lett.*, vol. 121, no. 4, p. 042105, Jul. 2022, doi: 10.1063/5.0097564.
- [21] W. Hao, Q. He, X. Zhou, X. Zhao, G. Xu, and S. Long, "2.6 kV NiO/Ga2O3 Heterojunction Diode with Superior High-Temperature Voltage Blocking Capability," in 2022 IEEE 34th International Symposium on Power Semiconductor Devices and ICs (ISPSD), May 2022, pp. 105–108, doi: 10.1109/ISPSD49238.2022.9813680.
- [22] J. Zhang, P. Dong, K. Dang, Y. Zhang, Q. Yan, H. Xiang, J. Su, Z. Liu, M. Si, J. Gao, M. Kong, H. Zhou, and Y. Hao, "Ultra-wide bandgap semiconductor Ga2O3 power diodes," *Nat. Commun.*, vol. 13, no. 1, p. 3900, Jul. 2022, doi: 10.1038/s41467-022-31664-y.
- [23] Y. Lv, Y. Wang, X. Fu, S. Dun, Z. Sun, H. Liu, X. Zhou, X. Song, K. Dang, S. Liang, J. Zhang, H. Zhou, Z. Feng, S. Cai, and Y. Hao, "Demonstration of β-Ga2O3 Junction Barrier Schottky Diodes With a Baliga's Figure of Merit of 0.85 GW/cm2 or a 5A/700 V Handling Capabilities," *IEEE Trans. Power Electron.*, vol. 36, no. 6, pp. 6179–6182, Jun. 2021, doi: 10.1109/TPEL.2020.3036442.
- [24] H. H. Gong, X. X. Yu, Y. Xu, X. H. Chen, Y. Kuang, Y. J. Lv, Y. Yang, F.-F. Ren, Z. H. Feng, S. L. Gu, Y. D. Zheng, R. Zhang, and J. D. Ye, "β-Ga2O3 vertical heterojunction barrier Schottky diodes terminated with p-NiO field limiting rings," *Appl. Phys. Lett.*, vol. 118, no. 20, p. 202102, May 2021, doi: 10.1063/5.0050919.
- [25] G. Feng, J. Suda, and T. Kimoto, "Space-Modulated Junction Termination Extension for Ultrahigh-Voltage p-i-n Diodes in 4H-SiC," *IEEE Trans. Electron Devices*, vol. 59, no. 2, pp. 414–418, Feb. 2012, doi: 10.1109/TED.2011.2175486.
- [26] W. Sung, A. Q. Huang, and B. J. Baliga, "Bevel Junction Termination Extension—A New Edge Termination Technique for 4H-SiC High-Voltage Devices," *IEEE Electron Device Lett.*, vol. 36, no. 6, pp. 594– 596, Jun. 2015, doi: 10.1109/LED.2015.2427654.
- [27] S. Nandy, B. Saha, M. K. Mitra, and K. K. Chattopadhyay, "Effect of oxygen partial pressure on the electrical and optical properties of highly (200) oriented p-type Ni1-xO films by DC sputtering," *J. Mater. Sci.*, vol. 42, no. 14, pp. 5766–5772, Jul. 2007, doi: 10.1007/s10853-006-1153-x.
- [28] M. Xiao, Y. Ma, K. Cheng, K. Liu, A. Xie, E. Beam, Y. Cao, and Y. Zhang, "3.3 kV Multi-Channel AlGaN/GaN Schottky Barrier Diodes With P-GaN Termination," *IEEE Electron Device Lett.*, vol. 41, no. 8, pp. 1177–1180, Aug. 2020, doi: 10.1109/LED.2020.3005934.
- [29] W. Li, D. Saraswat, Y. Long, K. Nomoto, D. Jena, and H. G. Xing, "Near-ideal reverse leakage current and practical maximum electric field in β-Ga2O3 Schottky barrier diodes," *Appl. Phys. Lett.*, vol. 116, no. 19, p. 192101, May 2020, doi: 10.1063/5.0007715.
- [30] H. Lawrence and R. M. Warner Jr., "Diffused Junction Depletion Layer Calculations," *Bell Syst. Tech. J.*, vol. 39, no. 2, pp. 389–403, 1960, doi: 10.1002/j.1538-7305.1960.tb01607.x.
- [31] Z. Hu, H. Zhou, Q. Feng, J. Zhang, C. Zhang, K. Dang, Y. Cai, Z. Feng, Y. Gao, X. Kang, and Y. Hao, "Field-Plated Lateral β-Ga2O3 Schottky Barrier Diode With High Reverse Blocking Voltage of More Than 3 kV and High DC Power Figure-of-Merit of 500 MW/cm2," *IEEE Electron Device Lett.*, vol. 39, no. 10, pp. 1564–1567, Oct. 2018, doi: 10.1109/LED.2018.2868444.